Supporting information for "Spectroscopic insight into molecular fluctuations and phase stability of nematic composites containing gold nanoparticles or carbon nanotubes"

Mathias Bourg and Martin Urbanski
Contact: Martin.Urbanski@lc-science.info

August 9, 2017

1 Orientational fluctuations of rod-shaped molecules in the isotropic and nematic state

Rod-shaped molecules in an isotropic liquid can undergo two principal relaxation modes: rotational fluctuations around the long molecular axis (see Figure 1 (a)) and reorientation fluctuations around the short molecular axis (Figure 1 (b)).

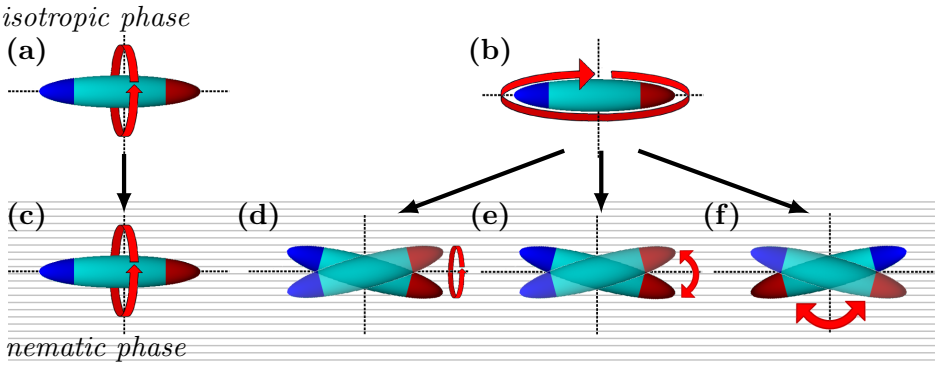

Figure 1: Schematic representation of possible orientational relaxation modes of rod-shaped molecules in an isotropic liquid ((a)+(b)) or nematic ((c)-(f)) phase. Redrawn from Yin et al.,[3] with kind permission of Springer.

Upon cooling into the nematic phase, the occurring uniaxial long-range orientational order imposes an additional potential onto the molecules.[1,2] Molecular fluctuations around the long molecular axis are barely affected by this nematic potential (compare Figure 1 (a) and (c)). However, in the nematic state the molecular relaxation mode accounting for reorientation fluctuations around the short molecular axis splits up into three new distinct modes.[3,4] Two of these three modes are tumbling modes and account for a precession (cf. Figure 1 (d)) or oscillation (cf. Figure 1 (e)) of molecules within one of the two potential wells (cf. Figure 2) described by the nematic potential, while the third mode accounts for a switching of molecular orientation between these two wells by rotational fluctuations around the molecules short axis (cf. Figure 1 (f)).[3,4] This latter mode (δ-relaxation) constitutes

the most prominent relaxation mode in nematics and is subject to experimental evaluation in this study. The δ-mode mainly contributes to $\epsilon_{\parallel}$ and its relaxation frequency f_δ occurs typically at several magnitudes lower frequencies than the tumbling modes due to its high activation energy.[5] The three tumbling fluctuations of molecules around their long axis mostly contribute to $\epsilon_{\perp}$, these modes exhibit relaxation frequencies comparable in magnitude which often form a single broad relaxation peak in the high MHz to GHz region of the dielectric spectrum.[5]

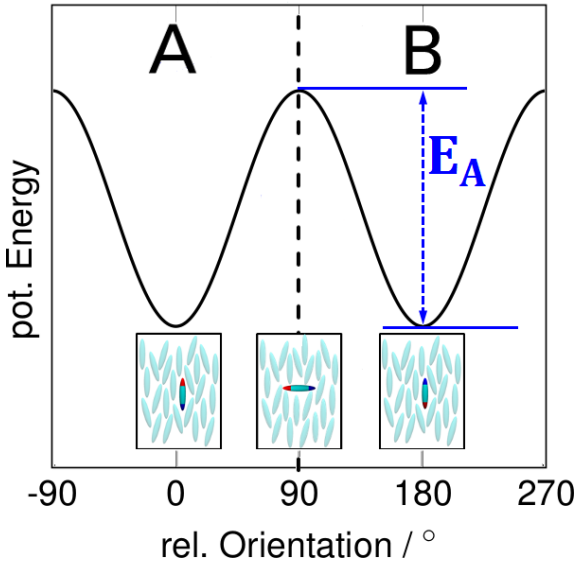

Figure 2: Schematic representation of the orientational potential of rod-shaped molecules in the nematic state. In equilibrium, molecules pointing upwards or downwards along the director $\hat{n}$ exhibit the same potential energy, while molecules oriented perpendicular to the local long-range orientational order exhibit a higher potential energy. The depth of the energy barrier E_A between these two states determines the rate r of molecular fluctuations between the two potential wells A and B. The orientational polarization in such system changes with twice the exchange rate r between the two potential wells, which leads to the relation $f_\delta = 2r$.

The potential well separating initial and final orientation of a fluctuating rod-shaped molecule rotating around its short molecular axis is well-defined by the uniaxial nematic order,[6] as illustrated in Figure 2. The local preferred direction along which the molecules in a nematic phase tend to align is given by the director $\hat{n}$, which is a signless pseudo-vector since $+\hat{n}$ and $-\hat{n}$ are indistinguishable. This indistinguishability arises from an equal number of molecules pointing *upwards* along the director (cf. potential well A in Figure 2) or pointing *downwards* along the director (cf. potential well B in Figure 2). In equilibrium, also the exchange rates of molecules between the two potential wells A and B, r_{AB} and r_{BA}, are equal and hence no net orientational polarization is present. Applying an external electric field $\vec{E}$ parallel to the director energetically favors molecular dipoles being oriented anti-parallel to the electric field, hence the population of the respective potential well rises while the population in the other well depletes. After switching off the external electric field again, the systems relaxes

towards the initial equilibrium condition with the relaxation frequency

$$f_\delta = \exp -\frac{q_N + q_{visc}}{k_B T}, \tag{1}$$

with q_N representing the anisotropic part of the potential barrier and q_{visc} representing the isotropic viscous part of the potential barrier, k_B being the Boltzmann constant and T the absolute temperature. The anisotropic part of the potential barrier, which arises from the uniaxial long-range order, strongly depends on the scalar order parameter S of the nematic phase via the relation $q_N = -1/2BS\left(3\cos^2\theta - 1\right)$, with B being a material parameter and θ being the angle between a molecules long axis and the local director $\hat{n}$. Hence, doping-induced changes in the relaxation frequency f_δ result from either changes in the viscous properties of the material or a change in the nematic order parameter.

2 Composition of the nematic mixture E7

The nematic mixture E7 used as a host material in the present study is composed of four cyano-biphenyl and -terphenyl compounds, as summarized in table 1:

Table 1: Overview of chemical structures and weight-% of the four compounds in the nematic mixture E7.

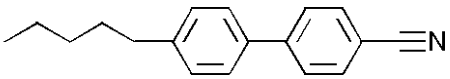

4-cyano-4'-n-pentyl-biphenyl **51.0 %**

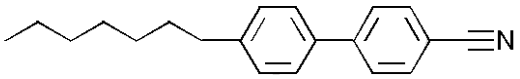

4-cyano-4'-n-heptyl-biphenyl **25.0 %**

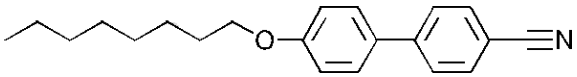

4-cyano-4'-n-oxyoctyl-biphenyl **16.0 %**

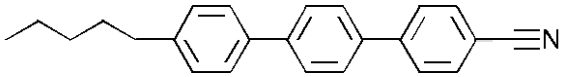

4-cyano-4"-n-pentyl-p-terphenyl **8.0 %**

3 Composition of gold nanoparticles NP1

Dodecanethiol-capped gold nanoparticles **NP1** exemplarily represent non-ferroelectric, spherical nanoparticles as dopants for nematic liquid crystals. The use of alkylthiol-functionalized nanoparticles is justified by the large number of experimental studies which successfully utilized particles with comparable particle size or surface functionalization. In the following section, we will briefly outline the role of particle size and surface functionalization and guide the interested reader towards respective seminal studies and review articles.

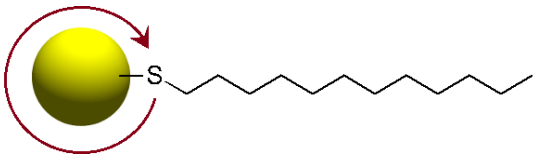

Figure 3: Schematic representation of the composition of **NP1**.

3.1 The role of nanoparticle size for interactions with the LC host

Depending on the spatial dimension of nanoparticles, the impact of dispersed particles on the uniaxial order of a nematic host can be distinguished into two regimes: (i) Large particles with $r_p >> K/W$ (r_p being the radius of the particle, K being the average Frank elastic constant and W being the anchoring energy at the nanoparticle-host interface) affect the director field in their vicinity and thereby induce topological defects into the uniaxial order of the nematic host.[7] (ii) Small particles with $r_p << K/W$, in the contrary, do not induce topological defects to the director field, their preferential surface anchoring is disregarded by the host phase. While the increase of the nematic elastic bulk free energy density scales with Kr_p, the energy required for a deviation from the particles preferred surface anchoring is proportional to Wr_p^2.[8] Consequently, for sufficiently small nanoparticles the energy required to form topological defects in the bulk exceeds the energy penalty for deviating from the preferred anchoring at the particles surface and no topological defects are formed.[9]
Nanoparticles with diameters of 3-5 nm as used in this present study qualify as *small particles*, since they do not induce topological defects to the director field of the nematic host phase. The NP-host interactions discussed in our manuscript do therefore not refer to interactions between single nanoparticles and the director $\hat{n}$ (which in the frame of continuums theory requires a large number of molecules to define the long-range orientational order of a nematic), but to interactions between single nanoparticle and the limited number of host molecules in their closest vicinity.
Changing the particle size within the regime of *small particles* is not expected to alter the main principle of interactions between nanoparticles and host molecules, but rather affects the number of interaction centers: If at a given doping concentration in % (w/w) the particle size is decreased, the number of nanoparticles in the dispersion rises. This would reduce the average distance between dispersed nanoparticles and increase the volume fraction of liquid crystal in the close vicinity to a nanoparticle. If the particle size increased, the number of nanoparticles would decrease and so would the volume fraction of liquid crystal molecules close to the dispersed nanoparticles.

3.2 The role of surface functionalization

Nanometer-sized metal nanoparticles are not particularly stable due to their high surface to volume ratio, but tend to aggregate and form larger clusters.[10,11] An organic capping layer of covalently bound molecules on the particles surface has been demonstrated a versatile method to prevent particle agglomeration and also represents a powerful method for increasing or fine-tuning the dispersibility of nanoparticles in a respective nematic host phase. Numerous studies in this field have shown that a structural similarity between ligand and host molecules is not required to chemically match the host phase and successfully prevent agglomeration.[12] However, a few particular structural properties have been found to be in particular suitable: The ligand molecules should be sufficiently long and flexible, so that they can adapt to the uniaxial order of the nematic host phase. As demonstrated by Draper and Goodby, the ligands of well-dispersible particles form rigid poles of unfolded ligand chains and a soft equator of folded ligand molecules, rendering the initially spherical ligand shell tactoidally deformed upon interaction with the nematic phase.[13] Furthermore, meso-

genic units linked to particle surface via flexible spacer molecules have often been utilized as suitable capping agents to increase the dispersibility.[12,14–16]
Experimental studies on the composition of either aliphatic or mesogenic functionalized gold nanoparticles showed that the ligand density on the particles surface is typically high, with 0.77-1.11 ligands per surface atom reported by Draper and Goodby[13,17] or 1.15-2.38 ligands per surface atom reported by Mirzaei and Hegmann.[18] Based on these findings, it is well accepted that the metal core is effectively shielded from interactions with the nematic host and that the dispersibility of particles in the respective host phase is driven by molecular interactions between ligand shell and host molecules.[9]

References

[1] G. Meier and A. Saupe, *Molecular Crystals*, 1966, **1**, 515–525.

[2] A. J. Martin, G. Meier and A. Saupe, *Symp. Farad. Soc.*, 1971, **5**, 119–133.

[3] Y. Yin, S. V. Shiyanovskii and O. D. Lavrentovich, in *Fast Switching of Nematic Liquid Crystals by an Electric Field: Effects of Dielectric Relaxation on the Director and Thermal Dynamics*, ed. A. Ramamoorthy, Springer Netherlands, Dordrecht, 2007, pp. 277–295.

[4] S. V. Shiyanovskii and O. D. Lavrentovich, *Liquid Crystals*, 2010, **37**, 737–745.

[5] A. R. Bras, M. Dionisio, H. Huth, C. Schick and A. Schoenhals, *Physical review. E, Statistical, nonlinear, and soft matter physics*, 2007, **75**, 061708.

[6] H. R. Zeller, *Phys. Rev. Lett.*, 1982, **48**, 334–338.

[7] D. Voloschenko, O. P. Pishnyak, S. V. Shiyanovskii and O. D. Lavrentovich, *Phys. Rev. E*, 2002, **65**, 060701.

[8] J.-C. Loudet, P. Barois and P. Poulin, *Nature*, 2000, **407**, 611–613.

[9] M. Urbanski, *Liquid Crystals Today*, 2015, **24**, 102–115.

[10] H. Qi, B. Kinkead, V. M. Marx, H. R. Zhang and T. Hegmann, *Chemphyschem : a European journal of chemical physics and physical chemistry*, 2009, **10**, 1211–1218.

[11] S. Saliba, C. Mingotaud, M. L. Kahn and J.-D. Marty, *Nanoscale*, 2013, **5**, 6641–6661.

[12] M. Baginski, A. Szmurlo, A. Andruszkiewicz, M. Wojcik and W. Lewandowski, *Liquid Crystals*, 2016, **43**, 2391–2409.

[13] M. Draper, I. M. Saez, S. J. Cowling, P. Gai, B. Heinrich, B. Donnio, D. Guillon and J. W. Goodby, *Advanced Functional Materials*, 2011, **21**, 1260–1278.

[14] L. Cseh and G. H. Mehl, *J. Mater. Chem.*, 2007, **17**, 311–315.

[15] X. Mang, X. Zeng, B. Tang, F. Liu, G. Ungar, R. Zhang, L. Cseh and G. H. Mehl, *Journal of Materials Chemistry*, 2012, **22**, 11101.

[16] W. Lewandowski, M. Wojcik and E. Gorecka, *Chemphyschem : a European journal of chemical physics and physical chemistry*, 2014, **15**, 1283–1295.

[17] Michael Draper, *PhD Thesis*, University of York, York, 2009.

[18] J. Mirzaei, M. Urbanski, H.-S. Kitzerow and T. Hegmann, *Chemphyschem : a European journal of chemical physics and physical chemistry*, 2014, **15**, 1381–1394.